

Ultrafast cascading theory of intersystem crossings in transition-metal complexes

Jun Chang, A. J. Fedro, and Michel van Veenendaal

Department of Physics, Northern Illinois University, De Kalb, Illinois 60115, USA

and Advanced Photon Source, Argonne National Laboratory, 9700 South Cass Avenue, Argonne, Illinois 60439, USA

(Received 17 May 2010; published 12 August 2010)

We investigate the cascade decay mechanism for ultrafast intersystem crossing mediated by the spin-orbit coupling in transition-metal complexes. A quantum-mechanical description of the cascading process that occurs after photoexcitation is presented. The conditions for ultrafast cascading are given, which relate the energy difference between the levels in the cascading process to the electron-phonon self energy. These limitations aid in the determination of the cascade path. For Fe^{2+} spin-crossover complexes, this leads to the conclusion that the ultrafast decay primarily occurs in the manifold of antibonding metal-to-ligand charge-transfer states. We also give an interpretation why some intermediate states are bypassed.

DOI: [10.1103/PhysRevB.82.075124](https://doi.org/10.1103/PhysRevB.82.075124)

PACS number(s): 78.47.J-, 82.50.-m, 82.37.Vb, 82.53.-k

I. INTRODUCTION

Cascade decay is a universal phenomenon associated with excited-state relaxation in photophysics and photochemistry. In most materials, the excited state that is reached after photoexcitation does not directly decay to the ground state but follows a complex route of intermediate states with often surprising changes in, e.g., spin and lattice parameters. The fastest cascading effects are generally associated with dephasing of states through the coupling to a continuum, e.g., Fano effects.¹ After the cascade, the system returns to the ground state or to a relatively long-lived metastable state. A highly complex example of cascading is photosynthetic water oxidation where multiple photoexcitations of a Mn_4Ca complex bound to amino acid residues in photosystem II leads to the production of O_2 from water molecules.² Obviously, a theoretical quantum-mechanical treatment of cascading is of the utmost importance but is also highly complex, and even many simpler systems are not well understood. A prototypical example of cascading occurs in spin-crossover phenomena in transition-metal complexes where photoexcitation of a low-spin ground state can lead to the creation of high-spin configurations on time scales as fast as several hundreds of femtosecond (fs). The reverse process has also been observed. Probably, the best-studied examples are Fe^{2+} complexes with a singlet t_{2g}^6 ground state (1A_1 in O_h symmetry) and a high-spin $t_{2g}^4 e_g^2$ (5T_2) configuration.³⁻¹² The relaxation from the metastable high-spin state to the ground state is slow with decay times ranging from nanosecond to days.

The advantage of studying the intersystem crossing in Fe compounds is that the cascading clearly involves two subsequent $t_{2g\downarrow} \rightarrow e_{g\uparrow}$ conversions. That this leads to an increase in the metal-ligand distance is well known since electrons in e_g orbitals repel the ligands more strongly than those in the t_{2g} orbitals. However, our understanding is complicated by the fact that excitations are not made into the local dd multiplets, which are generally well understood by *ab initio* techniques in the adiabatic limit^{13,14} but into the metal-to-ligand charge-transfer states. This makes the exact nature of the cascade path difficult to understand due to the competition between internal conversion between states of the same spin and intersystem crossings between states with different spin. Gen-

erally, the latter process is considered slower than the former. Furthermore, the decay is a nonadiabatic process requiring the relaxation of oscillations of vibronic states. This intramolecular vibrational energy redistribution is considered the fastest process.

In this paper, we first provide a quantum-mechanical cascade decay model for the photoinduced electron state in transition-metal complexes. A dissipative Schrödinger equation is introduced to include the effects of the interaction with the surroundings. In the case of Fe spin-crossover complexes, we propose a distinct and self-consistent photon-excited decay path, and find the cascade decay times in good agreement with experiments on the order of hundreds of femtosecond from the photoexcited singlet state to the quintet state. Although our decay times are in qualitative agreement with that of phenomenological rate equations, the more detailed understanding of the cascading allows a better identification of the states involved in the decay path and their time-dependent occupation than is possible with rate equations with constants inferred from experimental data.^{4,12}

II. CASCADE DECAY MODEL

In a cascading process, several levels at energies E_i are involved. The levels couple to the vibrational/phonon modes of energy $\hbar\omega$ of the surrounding ligands. Variations in coupling strength λ_i lead to different metal-ligand equilibrium distances for different states. The Hamiltonian is given by

$$H_s = \sum_i E_i n_i + \hbar\omega a^\dagger a + \lambda_i n_i (a^\dagger + a), \quad (1)$$

where n_i gives the occupation of state i and a^\dagger is the step operator for the vibrational mode. This Hamiltonian can be diagonalized with a unitary transformation $\bar{H}_s = e^S H_s e^{-S}$, with $S = \sum_i n_i \sqrt{g_i} (a^\dagger - a)$ and $g_i = \varepsilon_i / \hbar\omega$ with $\varepsilon_i = \lambda_i^2 / (\hbar\omega)$, giving,

$$\bar{H}_s = \sum_i (E_i - \varepsilon_i) n_i + \hbar\omega a^\dagger a \quad (2)$$

with eigenstates $|\psi_{in}\rangle$ for states i and n excited phonon modes. We define the energy difference between the states after diagonalization $\Delta_{ij} = (E_i - \varepsilon_i) - (E_j - \varepsilon_j)$. In addition,

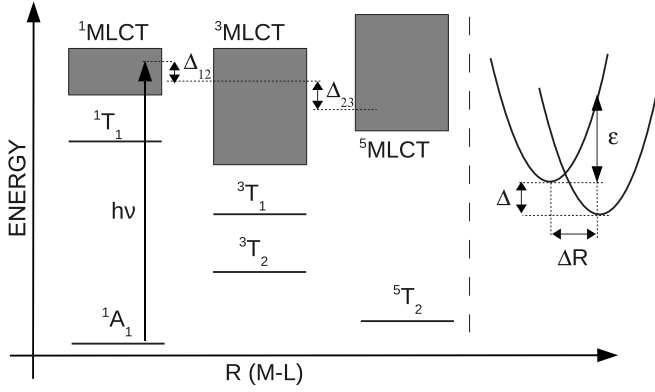


FIG. 1. Left plane: schematic energy-level scheme of Fe^{2+} -based complexes. The different configurations are given in octahedral notation. Manifolds of the MLCT states are indicated by the shadowed areas. Right plane: Δ , ε , and ΔR are the energy gap between the lowest vibrational levels, the electron-phonon self-energy difference, and the change in the equilibrium distance between two oscillation states, respectively.

since a spatial translation of the coordinates shifts all the λ_i by a constant in H_s , only the relative change in coupling is of importance. Therefore, it is useful to define the electron-phonon self-energy difference $\varepsilon_{ij} = (\lambda_i - \lambda_j)^2 / (\hbar\omega)$ between two different states (as shown in the right panel of Fig. 1). An interaction that cannot be diagonalized with the electron-phonon term is the spin-orbit coupling, which explains the prevalence of spin flips in many decay processes. This causes a coupling between different states,

$$H_I = \sum_{ij} V_{ij} (c_i^\dagger c_j + \text{H.c.}), \quad (3)$$

where V_{ij} is the coupling constant and $c_i^\dagger c_j$ causes a particle-conserving transition between states j and i . This “local” system is considered part of a larger system such as a molecule in solution or a solid. The latter constitute the effective surroundings that can dissipate energy from the local system. In the following, we demonstrate how to incorporate electronic and vibronic dissipation.

III. ENVIRONMENTAL DISSIPATION

The study of the dynamics of dissipative systems is notoriously difficult due to the absence of conservation of energy and/or particle number for the local system and the complex interaction with the environment. The density matrix method is a standard approach to dissipation problems.¹⁵ However, the density matrices may become unphysical under the perturbative expansion with respect to the system-bath coupling.¹⁶ Although Lindblad equations can solve this problem,¹⁷ a more serious disadvantage of the density-matrix technique is the difficulty in handling large systems. To reduce the calculation, a methodology that directly describes the nonequilibrium dynamics of the wave function is advantageous. For example, Strunz demonstrated that the dynamics of an open quantum system can be described by a non-Markovian stochastic Schrödinger equation.¹⁸ Here, we

describe a open quantum system with a dissipative Schrödinger equation for the system state $|\psi(t)\rangle$ which is given by

$$i\hbar \frac{d|\psi(t)\rangle}{dt} = (H_0 + iD)|\psi(t)\rangle, \quad (4)$$

where H_0 is the Hamiltonian of the system and D describes the effective environmental dissipation.

When selecting the basis, we write the system vector,

$$|\psi(t)\rangle = \sum_k c_k(t) |\psi_k\rangle \quad (5)$$

with the coefficient c_k in terms of an amplitude $a_k(t) = |c_k(t)|$ and a phase φ_k , or $c_k(t) = a_k(t)e^{i\varphi_k(t)}$. We can express the change in the coefficient due to the presence of the bath

$$\left. \frac{dc_k(t)}{dt} \right|_B = \left. \frac{da_k(t)}{dt} \right|_B e^{i\varphi_k(t)} + ia_k(t) e^{i\varphi_k(t)} \left. \frac{d\varphi_k(t)}{dt} \right|_B. \quad (6)$$

In general, the coupling to the environment affects both the probability and the phase of the system. The latter term gives the change in phase, which causes an embedding of the local system in its surroundings. Due to the complexity of the surroundings, the precise nature of this embedding is often very difficult and can usually only be taken into account in some effective way. Here, we assume that the phase of the local system is changed randomly by the large number of degrees of freedom of the surroundings which results in a total phase change close to zero according to the law of large numbers. We therefore only consider the changes in the probability by the environment. Now let us assume for the moment that we are able to determine an expression for the change in amplitude $P_k = a_k^2$ in a particular basis (e.g., in the absence of certain intersystem couplings),

$$\left. \frac{dP_k}{dt} \right|_B = 2a_k \left. \frac{da_k}{dt} \right|_B = f(\{P_{kj}\}), \quad (7)$$

where f is a function of the probabilities P_k . Below we give the explicit expression for the change in probabilities related to the damping of phonons. The change in the coefficient due to the bath is then given by

$$\left. \frac{dc_k}{dt} \right|_B = \frac{1}{2a_k} \left. \frac{dP_k}{dt} \right|_B e^{i\varphi_k} = \frac{1}{2} \left. \frac{d \ln P_k}{dt} \right|_B c_k. \quad (8)$$

This leads to a dissipative term in Eq. (4) given by

$$D = \frac{\hbar}{2} \sum_k \frac{d \ln P_k(t)}{dt} |\psi_k\rangle \langle \psi_k|. \quad (9)$$

The dissipation does not necessarily have to be diagonal. After deriving the diagonal dissipation in a particular basis, a unitary transformation to a different (more suitable) basis can be made. After deriving an expression for the dissipation in a particular basis set, we can solve the problem in the presence of intersystem couplings and dissipation.

In cascade decay model, the eigenvectors $|\psi_{in}\rangle$ of \bar{H}_s are selected as the basis. The vibrational cooling by the bath can be taken into account by the dissipative Schrödinger equation in Eq. (4) with H_0 substituted by $\bar{H}_s + \bar{H}_I$ and \bar{H}_I

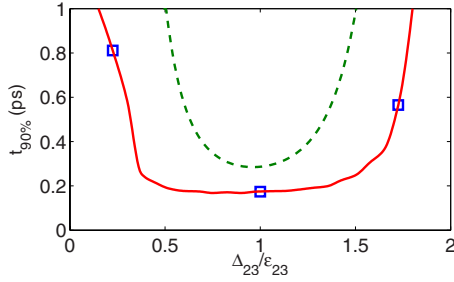


FIG. 2. (Color online) The time $t_{90\%}$ for the third state reaching its 90% population as a function of the energy difference between states 2 and 3 with $\Delta_{12}=\varepsilon_{12}=0.2$ eV and $\varepsilon_{23}=0.4$ eV. The solid (red) curve is calculated using the dissipative Schrödinger equation, the dashed (green) curve is based on rate equations with $t_{90\%}=-\ln 0.1/\gamma_0$ with $\gamma_0=\gamma_1\gamma_2/(\gamma_1+\gamma_2)$, $\gamma_{1,2}$ are defined in Eq. (12). For the values of Δ_{23} indicated by the squares, the time dependence is given in Fig. 3.

$=e^S H_i e^{-S}$. We still need the detailed formulae for Eq. (7). For state i with n excited phonon modes, on the one hand, the vibrational coupling to the surroundings relaxes a state with n phonons to a $n-1$ phonon state by the emission of phonons. On the other hand, the probability of the n -phonon state increases due to the decay of the state with $n+1$ phonons.^{19,20} This gives a change in the probability of the n -phonon state,

$$\frac{dP_{in}(t)}{dt} = -2n\Gamma P_{in}(t) + 2(n+1)\Gamma P_{i,n+1}, \quad (10)$$

where $P_{in}(t)=|\langle\psi_{in}|\psi(t)\rangle|^2$, $\Gamma=\pi\bar{\rho}\bar{V}^2/\hbar$ is the relaxation constant, where $\bar{\rho}$ is the effective bath phonon density of states and \bar{V} is the interaction between the local system and the bath. Due to the complication of \bar{V} , we take Γ as a parameter. Note that the decay time from state i to j is not directly related to Γ . Our numerical calculations are not sensitive to the change in $(2\Gamma)^{-1}$ from 20 to 60 fs. In Figs. 2 and 3, we take $(2\Gamma)^{-1}=30$ fs.

IV. IRON SPIN-CROSSOVER COMPLEXES

Let us specifically consider iron-based complexes, such as $\text{Fe}^{2+}(\text{bpy})_3$. A typical energy-level scheme is shown in Fig. 1. The Fe d^6 multiplet levels have been extensively studied. However, since these excitations are dipole forbidden, the system is often excited into so-called metal-to-ligand charge-transfer (MLCT) states. Spin crossovers are generally strongly covalent, where the metal states are given by $\alpha|d^6\rangle+\sum_i(\beta_i|d^7\bar{L}_i\rangle+\gamma_i|d^5L_i\rangle)+\dots$, where L_i and \bar{L}_i are an electron and a hole, respectively, on the ligand labeled i . The MLCT states are the antibonding states related to the metal states (e.g., ${}^1\text{MLCT}-{}^1A_1$, ${}^3\text{MLCT}-{}^3T_{1,2}$, and ${}^5\text{MLCT}-{}^5T_2$). Since the photoexcitation conserves spin, the initial photoexcited state starting from a 1A_1 ground state is the ${}^1\text{MLCT}$ state (with predominantly $t_{2g}^5e_g^1L^1$ character). A major problem in the identification of the states in the cascading process is that optical selection rules make it impossible to directly probe the intermediate states spectroscopically, and several

cascading paths to the metastable high-spin 5T_2 configuration have been proposed. McCusker *et al.*⁵ suggested that the ${}^1\text{MLCT}$ state directly decays to the high-spin 5T_2 quintet state requiring a spin change of $\Delta S=2$. Gawelda *et al.*⁸ proposed that the ${}^1\text{MLCT}$ state relaxes to the ${}^3\text{MLCT}$ within 30 fs followed by a departure from this state within ~ 120 fs. Subsequently, the quintet state is reached via intermediate ligand-field multiplets. Recently, Bressler *et al.*¹⁰ claimed that the ${}^3\text{MLCT}(t_{2g}^4e_g^1L^1)$ state directly relaxes to the 5T_2 state bypassing the ligand field triplet state. It is surprising that several states are bypassed, such as the triplet states ${}^3T_{1,2}$, which are located between the ${}^3\text{MLCT}$ and 5T_2 , and that there is no ${}^3\text{MLCT}$ to ${}^3T_{1,2}$ internal conversion, which is expected to occur on a faster time scale than the spin-crossover process. In order to understand the cascade process in Fe compounds, we first need to establish an appropriate range of parameters for Fe spin-crossover compounds. The strength of the interaction between the iron and its surrounding ligands can be obtained from *ab initio* calculations.¹⁴ The change in energy for different configurations is close to parabolic for an adiabatic change in the Fe-ligand distance. From the change in equilibrium distance, we can obtain a difference in electron-phonon coupling ε_{ij} of approximately $\varepsilon_{12}=0.2$ eV between the singlet and triplet state, and $\varepsilon_{23}=0.4$ eV between the triplet and quintet state. A typical energy for the Fe-ligand stretching mode is $\hbar\omega=30$ meV.²¹ Next, we need to determine the energies of the states involved in the cascading process. Since electronic transitions do not directly change the metal-ligand distance, an estimate of 2.6 eV can be obtained for the energy difference between the lowest vibrational levels of the ${}^1\text{MLCT}$ and 1A_1 states from the pump laser wavelength of 400 nm and the fluorescence of 600 nm from the lowest ${}^1\text{MLCT}$ state back to the 1A_1 state. Another weaker emission shows a shift to 660 nm corresponding to a change in energy of $\Delta_{12}=0.2$ eV.⁸ This small energy difference implies that state 2 is a ${}^3\text{MLCT}$ state,⁸ see Fig. 1. For the spin-orbital coupling, we take the atomic value for Fe, $V_{12}=V_{23}=0.05$ eV.

This leaves us with the question of the nature of the third state and how a complete relaxation to the lattice parameters of the quintet state can be observed within 300 fs. We can obtain more information on the energy of the level in the cascading process by solving the cascading equations given above for cascading from level 1 to level 3 via an intermediate level 2. We define i state occupation $P_i(t)=\sum_n P_{in}(t)$. Figure 2 shows the results for $t_{90\%}$, i.e., the time when the third level reaches its 90% population, as a function of Δ_{23} . The value of $t_{90\%}$ shows a broad minimum around $\Delta_{23}\cong\varepsilon_{23}\cong 0.4$ eV. The minimum calculated time to reach a 90% occupation of the third level in the cascading process is about 200 fs. This is in good agreement with the results by Bressler *et al.*¹⁰ that show that the metal-ligand distance reaches the high-spin value on the same time scale. Let us first note that $t_{90\%}$ increases rapidly when Δ_{23} is less than $0.3\varepsilon_{23}\cong 0.12$ eV or larger than $1.7\varepsilon_{23}\cong 0.68$ eV. This implies that the total energy bridged in the fast cascading process is at most $\Delta_{12}+\Delta_{23}\cong 0.32-0.88$ eV. This is insufficient to overcome the more than 1.8 eV energy gap between the initial photoexcited state and the 5T_2 high-spin state. Another possibility is that an internal conversion occurs between

states 2 and 3, for example, state 3 is a metal-centered ${}^3T_{1,2}$ triplet state, which are about 1 eV below state 2. For an internal conversion, the electron number of e_g orbitals is unchanged, and ε_{23} has to be less than ε_{12} which does involve a $t_{2g\uparrow} \rightarrow e_{g\downarrow}$ conversion. Using a reduced electron-phonon self-energy of ε_{23} of 0.2 eV while keeping $V_{23}=0.05$ eV, comparable results are obtained for the cascade time as a function of $\Delta_{23}/\varepsilon_{23}$ as in Fig. 2 (not shown). In order for the decay to occur in less than a picosecond, the energy gap between states 2 and 3 has to be less than $\sim 2\varepsilon_{23}=0.4$ eV. Therefore, even though the energy gap for an internal conversion is smaller so is the maximum energy difference for which we can have ultrafast decay, and can also rule out the metal-centered triplet states as the third state in the cascading process. This is in agreement with experiment, since the metal-ligand separation increases to 0.2 Å (Ref. 10) showing that the high-spin state is reached. Furthermore, many internal conversion processes are also bypassed. Since the ligands π^* orbitals are almost orthogonal to the metal e_g orbitals, the electrons at the ligand atoms can only return to the t_{2g} orbital. Therefore, this prohibits, for example, decay from the ${}^1\text{MLCT}$ ($t_{2g}^5L^1$) to the 1T_1 state ($t_{2g}^5e_g^1$). The only remaining possibility is that state 3 is a ${}^5\text{MLCT}$ ($t_{2g}^3e_g^2L^1$) state. Furthermore, in the broad ${}^5\text{MLCT}$ manifold, it is easier to find a level with $\Delta_{23} \approx \varepsilon_{23}$. This leads to the interesting conclusion that the entire ultrafast decay process occurs primarily in the antibonding MLCT states, a possibility not considered before. Subsequently, the ${}^5\text{MLCT}$ state can relax more slowly to the 5T_2 state through internal conversion, which is difficult to observe in extended x-ray-absorption fine structure experiments¹⁰ due to the comparable lattice parameters for the quintet states. This relaxation is slower since the spin-orbit coupling does not couple the two quintet states. Another reason that the ultrafast decay occurs in the MLCT states is that the broad manifold of MLCT states makes it easier to find states for which $\Delta_{ij} \approx \varepsilon_{ij}$ whereas for the ligand field multiplets, this condition is only satisfied accidentally. Therefore, for the first step in the cascade decay, it is not a coincidence that the strongest increase in intensity in the fluorescence occurs at $\Delta_{12} \approx 0.2$ eV,⁸ close to the value of ε_{12} although the energy of ${}^3\text{MLCT}$ manifold spans over 1.5 eV.

A qualitative understanding of the time dependence of the decay can be obtained starting from classical phenomenological rate equations,^{4,12}

$$\frac{dP_i(t)}{dt} = \gamma_{i-1}P_{i-1}(t) - \gamma_iP_i(t), \quad (11)$$

where $P_i(t)$ is the probability of i th level with $i=1 \dots N$. The rate constants γ_i can be calculated using Fermi's golden rule,^{22,23}

$$\gamma_i = 2\pi F_n V_{i,i+1}^2 / \hbar^2 \omega, \quad (12)$$

where $V_{i,i+1}$ is the interaction between levels and $F_n = e^{-g} g^n / n!$ is the Franck-Condon factor with $n \approx \Delta_{i,i+1} / \hbar \omega$; $g = \varepsilon_{i,i+1} / \hbar \omega$ is the Huang-Rhys factor. Solving the above equations, we can approximately write the occupation of the final level in the cascading,

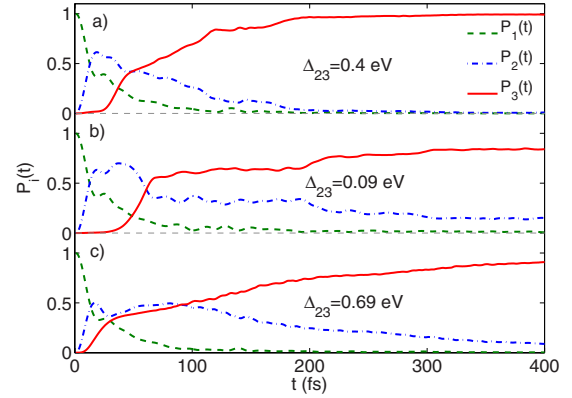


FIG. 3. (Color online) The probability of finding a particular state as a function of time for different values of Δ_{23} . The green dashed-dotted, the blue dashed, and the red solid curves give the probability of finding states 1, 2, and 3, respectively: (a) $\Delta_{23} = 0.4$ eV; (b) $\Delta_{23} = 0.09$ eV; (c) $\Delta_{23} = 0.69$ eV. Other parameters are the same as those in Fig. 2.

$$P_N(t) \approx 1 - e^{-\gamma_0 t} \quad (13)$$

with $1/\gamma_0 = \sum_{i=1}^{N-1} (1/\gamma_i)$. Figure 2 shows that, although rate equations give a qualitative description of $t_{90\%}$ as a function of $\Delta_{23}/\varepsilon_{23}$, quantitative differences are present. In the rate equation, energy conservation in Fermi's golden rule restricts the relaxation to states of equal energy whereas in the quantum-mechanical calculation, the state couples to the whole Franck-Condon continuum. This leads to a smaller minimum value for $t_{90\%}$ and also to a significantly broader minimum for the quantum-mechanical cascading process. The broad width of the minimum somewhat loosens the condition $\Delta_{ij} \approx \varepsilon_{23}$, which further explains the prevalence of ultrafast-decay processes.

For $\Delta_{23} = 0.4$ eV, we study the time-dependent occupations of the three states involved in the cascading process, see Fig. 3(a). We find that state 1 decays with a relaxation time about 20 fs. While the probability of state 2 increases quickly in the first 20 fs, it then begins to decrease due to relaxation into state 3. At 120 fs, it has lost most of its population, which agrees well with the experimentally observed departure from this state within ~ 120 fs.⁸ State 3 reaches almost 100% within 300 fs. All these time scales agree well with experiments.^{8,10} For $\Delta_{23} = 0.09$ eV and 0.69 eV, see Figs. 3(b) and 3(c), the decay of state 1 is almost the same as for $\Delta_{23} = 0.4$ eV, since the decay from $1 \rightarrow 2$ has been left unchanged, but the decay from state 2 has slowed down dramatically.

V. CONCLUSIONS

In conclusion, we have provided a quantum-mechanical model for the cascade decay mechanism of spin crossover in transition-metal complexes. Ultrafast cascading occurs when the energy difference between the levels is comparable to the self-energy ε . Since the latter is on the order of several hundreds meV, restrictions are imposed on the energy gap that can be bridged in the ultrafast cascading process. On the other hand, the manifold of the metal-to-ligand charge-

transfer states make the gaps between energy levels many and various. As a result, the ultrafast cascading in Fe spin-crossover complexes after excitation with visible light occurs primarily in these manifolds. We propose a distinct and self-consistent photon-excited decay path for $[\text{Fe}^{\text{II}}(\text{bpy})_3]^{2+}$, which is then ${}^1\text{MLCT} \rightarrow {}^3\text{MLCT} \rightarrow {}^5\text{MLCT} \rightarrow {}^5T_2 \rightarrow {}^1A_1$. Good agreement is found between the calculated and experimentally observed decay times. Our quantum model results qualitatively agree with the calculation of decay times based on the phenomenological rate equations combining with Franck-Condon factor. We further give an explanation why some intermediate states are bypassed.

ACKNOWLEDGMENTS

We are thankful to Xiaoyi Zhang and Yang Ding for helpful discussions. This work was supported by the U.S. Department of Energy (DOE), Office of Basic Energy Sciences, Division of Materials Sciences and Engineering under Award No. DE-FG02-03ER46097, and NIU's Institute for Nanoscience, Engineering, and Technology. Work at Argonne National Laboratory was supported by the U.S. DOE, Office of Science, Office of Basic Energy Sciences, under Contract No. DE-AC02-06CH11357.

-
- ¹U. Fano, *Phys. Rev.* **124**, 1866 (1961).
²See, e.g. H. Dau and M. Haumann, *Coord. Chem. Rev.* **252**, 273 (2008).
³S. Decurtins, P. Gütllich, K. M. Hasselbach, A. Hauser, and H. Spiering, *Inorg. Chem.* **24**, 2174 (1985).
⁴A. Hauser, *J. Chem. Phys.* **94**, 2741 (1991).
⁵J. K. McCusker, K. N. Walda, R. C. Dunn, J. D. Simon, D. Magde, and D. N. Hendrickson, *J. Am. Chem. Soc.* **115**, 298 (1993).
⁶P. Gütllich, A. Hauser, and H. Spiering, *Angew. Chem., Int. Ed. Engl.* **33**, 2024 (1994).
⁷W. Gawelda, V.-T. Pham, M. Benfatto, Y. Zaushitsyn, M. Kaiser, D. Grolimund, S. L. Johnson, R. Abela, A. Hauser, C. Bressler, and M. Chergui, *Phys. Rev. Lett.* **98**, 057401 (2007).
⁸W. Gawelda, A. Cannizzo, V. Pham, F. van Mouik, C. Bressler, and M. Chergui, *J. Am. Chem. Soc.* **129**, 8199 (2007).
⁹Y. Ogawa, S. Koshihara, K. Koshino, T. Ogawa, C. Urano, and H. Takagi, *Phys. Rev. Lett.* **84**, 3181 (2000).
¹⁰Ch. Bressler, C. Milne, V.-T. Pham, A. ElNahhas, R. M. Van der Veen, W. Gawelda, S. Johnson, P. Beaud, D. Grolimund, M. Kaiser, C. N. Borca, G. Ingold, R. Abela, and M. Chergui, *Science* **323**, 489 (2009).
¹¹A. D. Kirk, *Chem. Rev.* **99**, 1607 (1999).
¹²L. S. Forster, *Coord. Chem. Rev.* **227**, 59 (2002).
¹³N. Suaud, M.-L. Bonnet, C. Boilleau, P. Labéguerie, and N. Guihéry, *J. Am. Chem. Soc.* **131**, 715 (2009).
¹⁴B. Ordejón, C. de Graaf, and C. Sousa, *J. Am. Chem. Soc.* **130**, 13961 (2008).
¹⁵See, e.g., S. H. Lin, R. Alden, R. Islampour, H. Ma, and A. A. Villaeys, *Density Matrix Method and Femtosecond Processes* (World Scientific, Singapore, 1991).
¹⁶B. Palmieri, D. Abramavicius, and S. Mukamel, *J. Chem. Phys.* **130**, 204512 (2009).
¹⁷G. Lindblad, *Commun. Math. Phys.* **48**, 119 (1976).
¹⁸W. T. Strunz, *Dynamics of Dissipation*, Lecture Notes in Physics Vol. 597 (Springer-Verlag, Berlin, 2006), p. 377.
¹⁹F. Bopp, *Sitzungsber. Math. Naturwiss. Kl. Bayer. Akad. Wiss. München* **67**, 122 (1973); H. Dekker, *Phys. Rep.* **80**, 1 (1981).
²⁰M. van Veenendaal, J. Chang, and A. J. Fedro, *Phys. Rev. Lett.* **104**, 067401 (2010); M. Van Veenendaal, J. Chang, and A. Fedro, [arXiv:1005.1079](https://arxiv.org/abs/1005.1079) (unpublished).
²¹J. P. Tuchagues, A. Bousseksou, G. Molnár, J. J. McGarvey, and F. Varret, *Top. Curr. Chem.* **235**, 85 (2004).
²²J.-L. Brédas, D. Beljonne, V. Coropceanu, and J. Cornil, *Chem. Rev.* **104**, 4971 (2004).
²³K. Schmidt, S. Brovelli, V. Coropceanu, D. Beljonne, J. Cornil, C. Bazzini, T. Caronna, R. Tubino, F. Meinardi, Z. Shuai, and J.-L. Brédas, *J. Phys. Chem. A* **111**, 10490 (2007).